Flat Bands, Indirect Gaps, and Unconventional Spin-Wave Behavior Induced by a Periodic Dzyaloshinskii-Moriya Interaction

Gallardo, R. A.; Cortés-Ortuno, D.; Schneider, T.; Roldán-Molina, A.; Ma, F.; Lenz, K.; Fangohr, H.; Lindner, J.; Landeros, P.;

Originally published:

February 2019

Physical Review Letters 122(2019), 067204

DOI: https://doi.org/10.1103/PhysRevLett.122.067204

Chiral Magnonic Crystals: Unconventional Spin-Wave Phenomena Induced by a Periodic Dzyaloshinskii-Moriya Interaction

R. A. Gallardo,[1,2] D. Cortés-Ortuño,[3] T. Schneider,[4,5] A. Roldán-Molina,[6] Fusheng Ma,[7] R. E. Troncoso,[1,8] K. Lenz,[4] H. Fangohr,[3,9] J. Lindner,[4] and P. Landeros[1,2]

[1] *Departamento de Física, Universidad Técnica Federico Santa María, Avenida España 1680, Valparaíso, Chile*
[2] *Center for the Development of Nanoscience and Nanotechnology (CEDENNA), 917-0124 Santiago, Chile*
[3] *Faculty of Engineering and the Environment, University of Southampton, Southampton SO17 1BJ, United Kingdom*
[4] *Helmholtz-Zentrum Dresden – Rossendorf, Institut of Ion Beam Physics and Materials Research, Bautzner Landstr. 400, 01328 Dresden, Germany*
[5] *Department of Physics, Technische Universität Chemnitz, Reichenhainer Str. 70, 09126 Chemnitz, Germany*
[6] *Universidad de Aysén, Calle Obispo Vielmo 62, Coyhaique, Chile*
[7] *Magnetoelectronic Lab, School of Physics and Technology, Nanjing Normal University, Nanjing 210023, China*
[8] *Center for Quantum Spintronics, Department of Physics, Norwegian University of Science and Technology, NO-7491 Trondheim, Norway*
[9] *European XFEL GmbH, Holzkoppel 4, 22869 Schenefeld, Germany*

(Dated: May 16, 2018)

Periodically patterned metamaterials are known for exhibiting wave properties similar to the ones observed in electronic band structures in crystal lattices. In particular, periodic ferromagnetic materials, known as magnonic crystals, are characterized by the presence of bands and bandgaps in their spin-wave spectrum at tunable GHz frequencies. Recently, the fabrication of magnets hosting Dzyaloshinskii-Moriya interactions has been pursued with high interest since properties such as the stabilization of chiral spin textures and nonreciprocal spin-wave propagation emerge from this antisymmetric exchange coupling. In this context, to further engineer the magnonic band structure, we propose the implementation of magnonic crystals with periodic Dzyaloshinskii-Moriya interactions, which can be obtained, for instance, via patterning of periodic arrays of heavy-metals wires on top of an ultrathin magnetic film. We demonstrate through theoretical calculations and micromagnetic simulations that such systems show an unusual evolution of the standing spin waves around the gaps in areas of the film that are in contact with the heavy-metal wires. We also predict the emergence of flat magnonic bands and indirect gaps, demonstrating that these effects depend on the strength of the Dzyaloshinskii-Moriya interaction. This study opens new routes towards engineered magnonics for spin-wave-based devices.

Exotic wave phenomena observed in artificial periodic structures have made the study of metamaterials an active research field that spans different areas of condensed matter physics such as photonics, phononics, plasmonics, and magnonics [1–6]. In this context, photonic crystals lacking space-inversion and time-reversal symmetries were shown to exhibit nonreciprocal dispersions with interesting consequences, even in one-dimensional systems [7–10]. Magnetic metamaterials, referred to as magnonic crystals (MCs), are obtained by periodically modulating the properties of the host materials, which in turn enables the manipulation of spin wave (SW) dispersions [11–26]. Spin waves within magnonic crystals exhibit GHz frequencies with sub-micrometric wavelengths, which are significantly shorter than those of electromagnetic waves of the same frequency observed in photonic crystals [27]. For practical reasons, this important feature encourages the miniaturization of magnonic devices [28]. The design of MCs involve alternating materials, waveguides with variable width, nanowire arrays, antidot lattices [16–26] or surface modulated MCs [29–33]. Several Brillouin light scattering experiments, together with theoretical and numerical studies, have confirmed the presence of bandgaps in MCs [24–26]. The filtering of SWs at specific frequency ranges allows to perform logic operations, signal processing or the realization of magnon transistors, thus offering novel prospects for information and communication technologies [34–37]. Besides, nonreciprocal devices have the ability to transfer energy unidirectionally [38] and can be also used as microwave isolators and circulators [25, 39].

The theoretical prediction [40–42] and subsequent experimental probe of magnets with Dzyaloshinskii-Moriya interaction (DMI) enabled the observation of chiral spin textures such as helices, spirals and skyrmions in these materials [43–47]. Moreover, multiple studies have established that magnons are nonreciprocal in such systems [48–56], especially in thin ferromagnetic (FM) films next to a strong spin-orbit-coupling material, such as a heavy metal (HM), where the broken space-inversion symmetry at the interface induces an interfacial DMI [46, 47]. This fact, together with the broken time-reversal symmetry in actual ferromagnets, encourages to anticipate that a rich variety of physical phenomena arises from the combination of magnonics and interfacial DMI. For instance, unidirectional SW propagation in a narrow frequency band was shown in bi-component MCs

in contact with a HM layer [57]. The DMI also shifts the frequencies of the SW modes and increases the intensity of the absorption peaks of the calculated ferromagnetic resonance (FMR) spectrum of one-dimensional MCs [58]. Additional magnon modes in the FMR spectrum of FM/HM ellipses have been recently predicted using computer simulations, where the confinement creates a fixed nodal structure, generating an unusual SW behavior [59]. The nature of the magnon bands was theoretically discussed in an array of magnetic nanoislands on top of a HM layer, a system that admits for topologically nontrivial bands [60]. It was also argued that SWs can be amplified at the boundary between two regions with different DMI [61], while a similar system was considered to study domain wall motion [62]. Although these works highlight key aspects of the interplay between spin dynamics and DMI, exceptional features resulting from a *periodic* DMI have been overlooked so far.

In this letter, we study the role of a periodic interfacial DMI on the magnon band structure of thin magnetic films. We theoretically describe these systems with the plane-wave method [14] and using the MuMax3 [63] and OOMMF [64] micromagnetic codes [65]. We predict that a periodic modulation of the DMI strength induces three main effects: (i) Tunable indirect bandgaps, which are uniquely induced by the DMI, having a nonmonotonic dependence on its strength; (ii) Low-frequency flat magnonic bands, where the spin motions are strongly localized at the FM zones in contact with the HM, and (iii) An unconventional temporal evolution of the standing SWs in the areas with active DMI underneath the HM. While the indirect bandgap is expected due to the nonreciprocity, the time evolution of such modes is an uncommon phenomenon that, to our knowledge, has not been observed in other fields such as phononics or photonics. This effect implies that SWs have the ability to propagate in areas with active DMI and, at the same time, retain their standing wave character in the regions without DMI. The existence and further control of such a hybrid kind of wave, with both standing and propagating features, in turn could push magnonics further towards a new generation of information technologies.

The envisioned chiral magnonic crystals with a periodic DMI are illustrated in Fig. 1, where a thin FM film is covered with an array of HM wires, and a bi-component MC is coupled to a HM layer. Here, a is the periodicity and ℓ the width of the wires. We describe the SW dynamics using the Landau-Lifshitz equation taking into account exchange, dipolar, Zeeman and Dzyaloshinskii-Moriya interactions. According to Bloch's theorem and assuming SWs propagating along z, the dynamic magnetization (together with the saturation magnetization M_s, exchange length λ, and Dzyaloshinskii-Moriya constant D) is expanded into a Fourier series [65]. Since the DMI depends on the position along z, the derivation of the corresponding field included in the equation of motion requires a careful analysis, which can be found in Sec. S1 [65]. For the MC shown in Fig. 1(a), we use a $d = 3$ nm thick permalloy ($Ni_{80}Fe_{20}$) film with parameters $M_s = 658\,\mathrm{kA/m}$, $\lambda = 6.39\,\mathrm{nm}$, and gyromagnetic ratio $\gamma = 0.017587\,\mathrm{GHz/G}$. Additionally, we solve the SW modes through micromagnetic simulations (see Sec. S2 in [65]) for the systems proposed in Fig. 1.

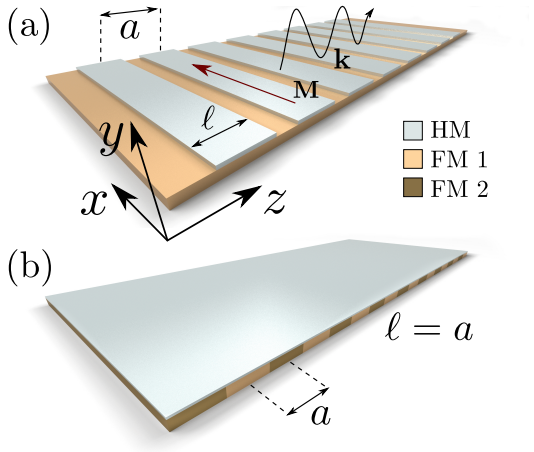

FIG. 1. Illustration of two possible realizations of a chiral magnonic crystal where spin waves propagate along z and the equilibrium magnetization points along x. (a) A ferromagnetic ultrathin film covered with an array of heavy-metal wires. (b) A bicomponent MC composed of FM 1 and FM 2 coupled to a HM layer. Both systems induce a periodic Dzyaloshinskii-Moriya coupling at the interfaces.

SW dispersion curves are shown in Fig. 2(a-b) for an FM film coupled with HM wires for $a = 100\,\mathrm{nm}$ and $\ell = a/2$, while $D = 1.5$ and $3\,\mathrm{mJ/m^2}$, which are close to experimental values [55, 56]. A bias field $\mu_0 H = 250\,\mathrm{mT}$ is applied along the HM stripes. The intensity plots in the background are the results from MuMax3 simulations whilst the lines correspond to the theory, where we have labeled the frequency branches as $\mathcal{B}^{\mathrm{I}}$, $\mathcal{B}^{\mathrm{II}}$, etc. In the case $D = 0$ (see Fig. S2(b) in [65]), the SW dispersion is reciprocal with the lowest frequency $f \approx 14.6$ GHz at $k = 0$. Increasing D, the SW dispersion becomes nonreciprocal, magnonic gaps open due to the periodic DMI, and the bottom of the SW dispersion shifts down in frequency and towards higher wave-vectors for $k > 0$ [66]. Interestingly, indirect bandgaps emerge out of the edges of the Brillouin zones (BZs), which are denoted by vertical dashed lines in Fig. 2. Indirect bandgaps induced by the inhomogeneous distribution of the surface SW intensity across the thickness, have been reported on thick metallized MCs [67–69]. Indirect bandgaps are due to nonreciprocity, since different wavelengths of two counter-propagating SWs shift the minimum and maximum of a given branch out of the borders of the BZs. For $D > 0$, the maximum of the 1st branch ($\mathcal{B}^{\mathrm{I}}_{\mathrm{max}}$) and the minimum of the 2nd branch ($\mathcal{B}^{\mathrm{II}}_{\mathrm{min}}$) move to the right,

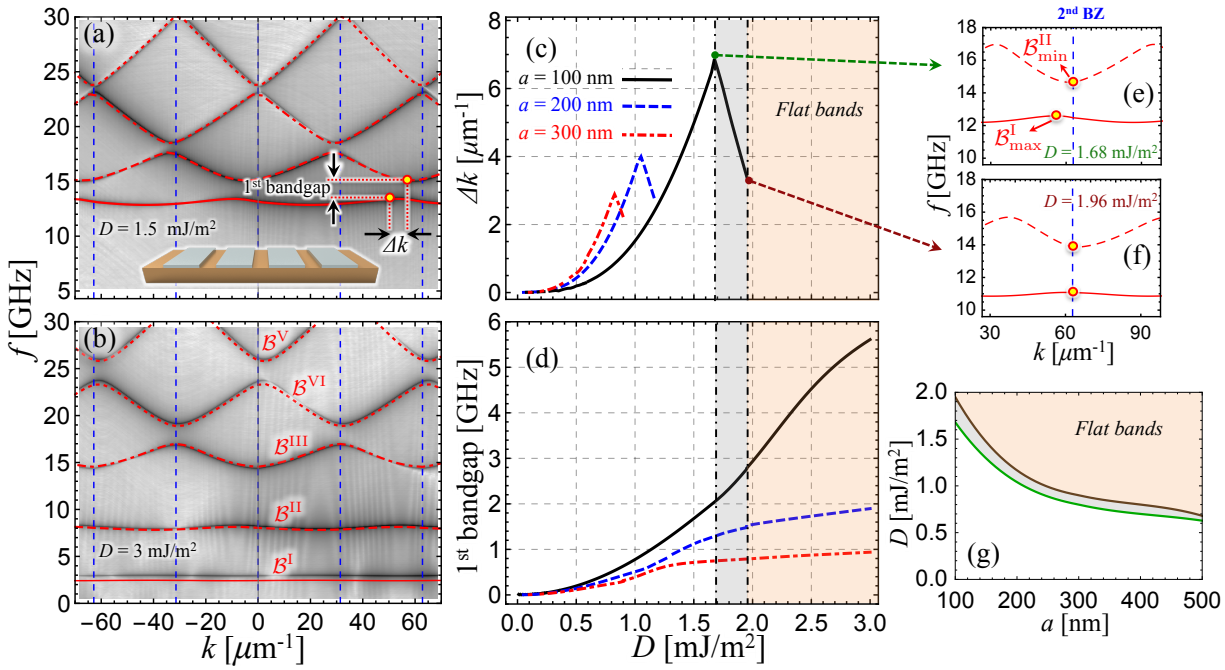

FIG. 2. (a,b) Illustration of the magnon band structure for a $Ni_{80}Fe_{20}$ film covered with a Pt wire array, where $a = 100$ nm, $D = 1.5$ and 3 mJ/m^2. The lines correspond to the theory and the color code represents the MuMax3 simulations; lighter (darker) color represents an intensity maximum (minimum). (c,d) Depicts the wavevector shift Δk and the 1st bandgap as a function of D, where the solid, dashed, dot-dashed lines show the cases $a = 100$, 200 and 300 nm, respectively. The shaded areas correspond to three ranges of D-values where different behaviors are predicted. (e,f) The first two branches at the critical values $D = 1.68$ and 1.96 mJ/m^2, for $a = 100$ nm. In (g) the three regions of D-values are shown as a function of a.

but in a different way, which gives rise to the indirect bandgaps. The same behavior was obtained using the OOMMF code (see Fig. S2 in [65]).

The behavior of the indirect bandgaps with respect to the DMI strength is shown in Fig. 2(c). Here, the wavevector separation Δk between the k-values at the minimum of $\mathcal{B}^{II}$ and maximum of $\mathcal{B}^{I}$, evidence a non-monotonic response with D. We use $\ell = a/2$ with $a =$ 100, 200 and 300 nm. Further, in Fig. 2(d) we plot the 1st bandgap (defined in Figs. 2(e-f) by $\mathcal{B}^{II}_{min}$ and $\mathcal{B}^{I}_{max}$), which clearly increases with D. The behavior of Δk observed in Fig. 2(c) motivates us to define three ranges of D: weak (white region), intermediate (gray region), and strong (flat bands region). The boundaries between these values depend on periodicity and have been highlighted just for $a = 100$ nm in Figs. 2(c,d). For weak D, Δk and the gap increase with it, up to $D \approx 1.68$ mJ/m^2, where $\mathcal{B}^{II}_{min}$ reaches the second BZ and remains pinned at its corresponding k value [see Fig. 2(e)]. In the intermediate region ($1.68 < D < 1.96$ mJ/m^2), $\mathcal{B}^{II}_{min}$ still remains pinned at the 2nd BZ while $\mathcal{B}^{I}_{max}$ moves towards the 2nd BZ. This explains the evident reduction of Δk in the gray region of Fig. 2(c). Once $\mathcal{B}^{I}_{max}$ reaches the 2nd BZ [see Fig. 2(f)], the first branch $\mathcal{B}^{I}$ becomes flat and defines the strong D-range. If D further increases, the upper-frequency branches also become flat [70]. For other periodicities, the boundaries between such D-values are displayed in Fig. 2(g), where the reduction of these boundaries with increasing periodicity becomes evident. The latter implies that larger periodicities favors the formation of flat bands, while shorter periodicities induce larger values of Δk. Since the flat modes exhibit a significant intensity in a broad k-range, they should be observed by inelastic light scattering as well as FMR measurements. Although it has been predicted that for uniformly magnetized infinite thin films the DMI does not affect the FMR mode [51], under the influence of a periodic DMI the FMR modes are clearly modified [58].

It has been previously established that the periodicity of the internal field in a MC, which gives rise to counter-propagating "Bragg-reflected" waves, induces frequency bandgaps [71], where the superposition of two opposing waves creates standing SWs around the BZs. However, in chiral MCs two counterpropagating SWs excited at the same frequency have different wavelengths, and therefore neither standing SWs nor bandgaps appear at the BZ edges, as shown in Fig. 2(a-b). Accordingly, the time evolution of the flat SW modes and the ones around the gaps are highly nontrivial and endemic of the periodic DMI. We emphasize this feature in Fig. 3, plotting the evolution of the dynamic magnetization component m_x for different modes and values of D. Figs. 3(a,b) correspond to modes $\mathcal{B}^{I}_{max}$ and $\mathcal{B}^{II}_{min}$, for $D = 1.5$ mJ/m^2. These modes are neither symmetric nor antisymmetric

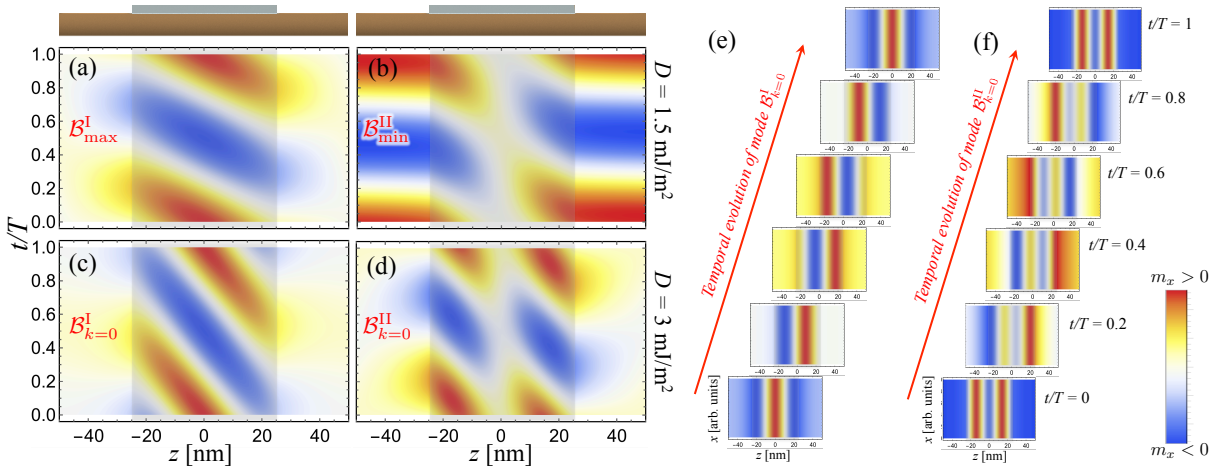

FIG. 3. Temporal and spatial evolution of the spin-wave modes, where T is the period of the oscillation. (a,b) Profiles of modes $\mathcal{B}^{\rm I}_{\rm max}$ and $\mathcal{B}^{\rm II}_{\rm min}$, for $D = 1.5$ mJ/m^2. (c,d) Mode profiles for the flat bands $\mathcal{B}^{\rm I}$ and $\mathcal{B}^{\rm II}$ evaluated at $k = 0$ for $D = 3$ mJ/m^2. (e,f) Snapshots of the temporal evolution of modes $\mathcal{B}^{\rm I}_{k=0}$ and $\mathcal{B}^{\rm II}_{k=0}$.

and correspond to standing SWs with local phase shifts. The dephasing occurs underneath the HMs, which in turn induces a nontrivial evolution of the magnetization displayed in Fig. 3. Below the HM wires (shaded area) the nonreciprocal nature of the coupling creates modes with nonzero phase velocities, i.e., waves that propagate inside the regions with active DMI. In contrast, a trivial standing character is observed outside these regions, hence the group velocities of the corresponding modes are zero. A similar behavior has been recently reported in confined elliptical nanostructures having DMI, where the FMR response was studied via micromagnetic simulations [59].

In Figs. 3(c,d), the SW profiles of the flat modes $\mathcal{B}^{\rm I}_{k=0}$ and $\mathcal{B}^{\rm II}_{k=0}$, are depicted for $D = 3\,\mathrm{mJ/m^2}$. Although these modes are evaluated at $k = 0$, it can be shown that their profiles are independent of k. We also observe nonzero phase velocities in the zones with active DMI, while the SW amplitudes are reduced in the regions without DMI. The time evolution of both modes is shown in Figs. 3(e,f), where the propagating character in the region with active DMI can be distinguished. Note that the slopes in the spatio-temporal plots shown in Fig. 3(a-d) increases with D and are zero for $D = 0$. This feature can be understood assuming a weak DMI strength as follows: since standing SWs are the superposition of two opposing waves, in the region where the DMI is nonzero, the right wavevector has the form $k_R = k + k'$, while the left one is $k_L = -(k - k')$. Thus, the wavevector shift is $k' \propto D$ [59]. Due to the constant slope in the t/T vs. z plots, the phase velocity of the SWs underneath the HMs is simply $v_p = \Delta z/t$. Then, taking into account that $v_p = \omega/k'$, one can show that $\frac{t/T}{\Delta z} \propto D$, where T is the period. Then, the slopes in Fig. 3(a-d) become larger as D increases.

The modulation of the band structure of the magnonic system can be reached through the change of the HM width. Alternatively, this can be obtained by using a bicomponent MC in contact with a continuous HM film (see Fig. 1b). For the former case, we show in Fig. S2 [65] that as the HM width increases, the first SW modes decrease in frequency and become flat. In the case of the bicomponent MC it is also possible to observe the emergence of flat bands. However, indirect bandgaps are not distinguishable due to the large value of D used, as shown in Fig. S5 [65]. For both kind of chiral MCs, results are predicted from the theory and substantiated with OOMMF and MuMax3 simulations.

In summary, we have predicted remarkable effects driven by a periodic Dzyaloshinskii-Moriya coupling. We highlight the formation of indirect bandgaps, the nontrivial temporal evolution of standing spin waves around the bandgaps, and the formation of low-frequency flat bands. This has been achieved using micromagnetic simulations and developing a theoretical approach based on the plane-wave method, which describes the dynamic properties of magnonic systems with incorporated periodic interfacial DMI. The occurrence of indirect gaps is a consequence of the nonreciprocal nature of the SWs caused by DMI, and occurs for D smaller than a critical value that depends on the periodicity. For stronger D, we found flat magnonic bands that should be observable by Brillouin light scattering as well as FMR measurements. Nonreciprocity also produces an unconventional temporal behavior of the SWs, with standing waves exhibiting finite phase velocities in the regions where the DMI is nonzero. We have demonstrated that chiral magnonic crystals host interesting fundamental physics and, for practical purposes, provide new routes for the field of magnonic metamaterials. We believe they can guide and encourage future experimental studies to prove and evidence these phenomena.

This work was supported by FONDECYT 11170736,

1161403, 3170647, CONICYT PAI/ACADEMIA 79140033, CONICYT Becas Chile 72140061, and Centers of excellence with Basal/CONICYT financing, grant FB0807, CEDENNA. D. C.-O. and H. F. acknowledge the EPSRC Programme grant on Skyrmionics (EP/N032128/1) and EPSRCs Doctoral Training Centre in Complex System Simulation (EP/G03690X/1). T.S. acknowledges funding from the InProTUC scholarship.

[1] N. I. Zheludev and Y. S. Kivshar, Nat. Mater. **11**, 917 (2012).
[2] O. Hess, J. B. Pendry, S. A. Maier, R. F. Oulton, J. M. Hamm, and K. L. Tsakmakidis, Nat. Mater. **11**, 573 (2012).
[3] M. Maldovan, Nature **503**, 209 (2013).
[4] H. Yu, G. Duerr, R. Huber, M. Bahr, T. Schwarze, F. Brandl, and D. Grundler, Nat. Commun. **4** (2013).
[5] A. V. Chumak, V. I. Vasyuchka, A. A. Serga, and B. Hillebrands, Nat. Phys. **11**, 453 (2015).
[6] P. Lodahl, S. Mahmoodian, S. Stobbe, A. Rauschenbeutel, P. Schneeweiss, J. Volz, H. Pichler, and P. Zoller, Nature **541**, 473 (2017).
[7] O. S. Eritsyan, J. Exp. Theor. Phys. **90**, 102 (2000).
[8] C. Koerdt, G. Düchs, and G. L. J. A. Rikken, Phys. Rev. Lett. **91**, 073902 (2003).
[9] A. H. Gevorgyan, Mol. Cryst. Liq. Cryst **382**, 1 (2002).
[10] I. Bita and E. L. Thomas, Proc. SPIE **5733**, 1 (2005).
[11] J. O. Vasseur, L. Dobrzynski, B. Djafari-Rouhani, and H. Puszkarski, Phys. Rev. B **54**, 1043 (1996).
[12] S. A. Nikitov, P. Tailhades, and C. S. Tsai, J. Magn. Magn. Mater. **236**, 320 (2001).
[13] V. V. Kruglyak and R. J. Hicken, J. Magn. Magn. Mater. **306**, 191 (2006).
[14] M. Krawczyk and H. Puszkarski, Phys. Rev. B **77**, 054437 (2008).
[15] K.-S. Lee, D.-S. Han, and S.-K. Kim, Phys. Rev. Lett. **102**, 127202 (2009).
[16] S. Neusser and D. Grundler, Adv. Mater. **21**, 2927 (2009).
[17] V. V. Kruglyak, S. O. Demokritov, and D. Grundler, J. Phys. D: Appl. Phys. **43**, 264001 (2010).
[18] A. A. Serga, A. V. Chumak, and B. Hillebrands, J. Phys. D: Appl. Phys. **43**, 264002 (2010).
[19] G. Gubbiotti, S. Tacchi, M. Madami, G. Carlotti, A. O. Adeyeye, and M. Kostylev, J. Phys. D: Appl. Phys. **43**, 264003 (2010).
[20] S.-K. Kim, J. Phys. D: Appl. Phys. **43**, 264004 (2010).
[21] Z. K. Wang, V. L. Zhang, H. S. Lim, S. C. Ng, M. H. Kuok, S. Jain, and A. O. Adeyeye, ACS Nano **4**, 643 (2010).
[22] A. Khitun, M. Bao, and K. L. Wang, J. Phys. D: Appl. Phys. **43**, 264005 (2010).
[23] B. Lenk, H. Ulrichs, F. Garbs, and M. Münzenberg, Phys. Rep. **507**, 107 (2011).
[24] S. O. Demokritov and A. N. Slavin, *Magnonics: From Fundamentals to Applications*, Top. Appl. Phys. (Springer Berlin Heidelberg, 2012).
[25] M. Krawczyk and D. Grundler, J. Phys.: Condens. Matter **26**, 123202 (2014).
[26] S. Tacchi, G. Gubbiotti, M. Madami, and G. Carlotti, J. Phys.: Condens. Matter **29**, 073001 (2017).
[27] J. D. Joannopoulos, S. G. Johnson, J. N. Winn, and R. D. Meade, *Photonic crystals: molding the flow of light* (Princeton university press, 2011).
[28] S. Tacchi, P. Gruszecki, M. Madami, G. Carlotti, J. W. Kłos, M. Krawczyk, A. Adeyeye, and G. Gubbiotti, Sci. Rep. **5**, 10367 (2015).
[29] I. Barsukov, F. M. Römer, R. Meckenstock, K. Lenz, J. Lindner, S. Hemken to Krax, A. Banholzer, M. Körner, J. Grebing, J. Fassbender, and M. Farle, Phys. Rev. B **84**, 140410 (2011).
[30] P. Landeros and D. L. Mills, Phys. Rev. B **85**, 054424 (2012).
[31] B. Obry, P. Pirro, T. Brächer, A. V. Chumak, J. Osten, F. Ciubotaru, A. A. Serga, J. Fassbender, and B. Hillebrands, Appl. Phys. Lett. **102**, 202403 (2013).
[32] R. A. Gallardo, A. Banholzer, K. Wagner, M. Körner, K. Lenz, M. Farle, J. Lindner, J. Fassbender, and P. Landeros, New J. Phys. **16**, 023015 (2014).
[33] M. Langer, F. Röder, R. A. Gallardo, T. Schneider, S. Stienen, C. Gatel, R. Hübner, L. Bischoff, K. Lenz, J. Lindner, P. Landeros, and J. Fassbender, Phys. Rev. B **95**, 184405 (2017).
[34] A. Khitun and K. L. Wang, Superlattice. Microst. **38**, 184 (2005).
[35] M. Jamali, J. H. Kwon, S.-M. Seo, K.-J. Lee, and H. Yang, Sci. Rep. **3** (2013).
[36] S.-K. Kim, K.-S. Lee, and D.-S. Han, Appl. Phys. Lett. **95**, 082507 (2009).
[37] A. V. Chumak, A. A. Serga, and B. Hillebrands, Nat. Commun. **5** (2014).
[38] T. An, V. I. Vasyuchka, K. Uchida, A. V. Chumak, K. Yamaguchi, K. Harii, J. Ohe, M. B. Jungfleisch, Y. Kajiwara, H. Adachi, B. Hillebrands, S. Maekawa, and E. Saitoh, Nat. Mater. **12**, 549 (2013).
[39] R. Verba, V. Tiberkevich, E. Bankowski, T. Meitzler, G. Melkov, and A. Slavin, Appl. Phys. Lett. **103**, 082407 (2013).
[40] I. Dzyaloshinsky, J. Phys. Chem. Solids **4**, 241 (1958).
[41] T. Moriya, Phys. Rev. Lett. **4**, 228 (1960).
[42] A. Fert and P. M. Levy, Phys. Rev. Lett. **44**, 1538 (1980).
[43] U. K. Rößler, A. N. Bogdanov, and C. Pfleiderer, Nature **442**, 797 (2006).
[44] S. Mühlbauer, B. Binz, F. Jonietz, C. Pfleiderer, A. Rosch, A. Neubauer, R. Georgii, and P. Böni, Science **323**, 915 (2009).
[45] N. Nagaosa and Y. Tokura, Nat. Nanotech. **8**, 899 (2013).
[46] R. Wiesendanger, Nat. Rev. Mater. **1**, 16044 (2016).
[47] A. Fert, N. Reyren, and V. Cros, Nat. Rev. Mater. **2**, 17031 (2017).
[48] L. Udvardi and L. Szunyogh, Phys. Rev. Lett. **102**, 207204 (2009).
[49] K. Zakeri, Y. Zhang, J. Prokop, T.-H. Chuang, N. Sakr, W. X. Tang, and J. Kirschner, Phys. Rev. Lett. **104**, 137203 (2010).
[50] A. T. Costa, R. B. Muniz, S. Lounis, A. B. Klautau, and D. L. Mills, Phys. Rev. B **82**, 014428 (2010).
[51] D. Cortés-Ortuño and P. Landeros, J. Phys.: Condens. Matter **25**, 156001 (2013).
[52] K. Di, V. L. Zhang, H. S. Lim, S. C. Ng, M. H. Kuok, J. Yu, J. Yoon, X. Qiu, and H. Yang, Phys. Rev. Lett. **114**, 047201 (2015).
[53] J. Cho, N.-H. Kim, S. Lee, J.-S. Kim, R. Lavrijsen,

A. Solignac, Y. Yin, D.-S. Han, N. J. J. van Hoof, H. J. M. Swagten, B. Koopmans, and C.-Y. You, Nat. Commun. **6** (2015).
[54] H. T. Nembach, J. M. Shaw, M. Weiler, E. Jue, and T. J. Silva, Nat. Phys. **11**, 825 (2015).
[55] M. Belmeguenai, J.-P. Adam, Y. Roussigné, S. Eimer, T. Devolder, J.-V. Kim, S. M. Cherif, A. Stashkevich, and A. Thiaville, Phys. Rev. B **91**, 180405 (2015).
[56] S. Tacchi, R. E. Troncoso, M. Ahlberg, G. Gubbiotti, M. Madami, J. Åkerman, and P. Landeros, Phys. Rev. Lett. **118**, 147201 (2017).
[57] F. Ma and Y. Zhou, RSC Adv. **4**, 46454 (2014).
[58] M. Mruczkiewicz and M. Krawczyk, Phys. Rev. B **94**, 024434 (2016).
[59] B. V. Zingsem, M. Farle, R. L. Stamps, and R. E. Camley, arXiv:1609.03417 (2017).
[60] E. Iacocca and O. Heinonen, Phys. Rev. Appl. **8**, 034015 (2017).
[61] S.-J. Lee, J.-H. Moon, H.-W. Lee, and K.-J. Lee, Phys. Rev. B **96**, 184433 (2017).
[62] I.-S. Hong, S.-W. Lee, and K.-J. Lee, Curr. Appl. Phys. **17**, 1576 (2017).
[63] A. Vansteenkiste, J. Leliaert, M. Dvornik, M. Helsen, F. Garcia-Sanchez, and B. Van Waeyenberge, AIP Advances **4**, 107133 (2014).
[64] M. J. Donahue and D. G. Porter, "Oommf user's guide, version 1.0," in *Interagency Report NISTIR 6376* (National Institute of Standards and Technology, Gaithersburg, MD, 1999).
[65] See Supplemental Material [url], which includes Refs. [] .
[66] Note that the $k = 0$ state does not change its frequency with D, but the group velocity does.
[67] M. Mruczkiewicz, M. Krawczyk, G. Gubbiotti, S. Tacchi, Y. A. Filimonov, D. V. Kalyabin, I. V. Lisenkov, and S. A. Nikitov, New J. Phys. **15**, 113023 (2013).
[68] M. Mruczkiewicz, E. S. Pavlov, S. L. Vysotsky, M. Krawczyk, Y. A. Filimonov, and S. A. Nikitov, Phys. Rev. B **90**, 174416 (2014).
[69] V. D. Bessonov, M. Mruczkiewicz, R. Gieniusz, U. Guzowska, A. Maziewski, A. I. Stognij, and M. Krawczyk, Phys. Rev. B **91**, 104421 (2015).
[70] That is the reason why Δk is not shown for strong D in Fig. 2(c), where the branch $\mathcal{B}^{\mathrm{I}}$ basically does not have a maximum and hence, Δk is not well defined.
[71] R. Zivieri, S. Tacchi, F. Montoncello, L. Giovannini, F. Nizzoli, M. Madami, G. Gubbiotti, G. Carlotti, S. Neusser, G. Duerr, and D. Grundler, Phys. Rev. B **85**, 012403 (2012).